Analyst

ROYAL SOCIETY OF CHEMISTRY

PAPER

View Article Online
View Journal | View Issue

Cite this: *Analyst*, 2022, **147**, 625

Multiplex digital PCR with digital melting curve analysis on a self-partitioning SlipChip†

Yan Yu,[a] Ziqing Yu,[a] Xufeng Pan,[b] Lei Xu,[a] Rui Guo,[a] Xiaohua Qian[a] and Feng Shen *[a]

Digital polymerase chain reaction (digital PCR) can provide absolute quantification of target nucleic acids with high sensitivity, excellent precision, and superior resolution. Digital PCR has broad applications in both life science research and clinical molecular diagnostics. However, limited by current fluorescence imaging methods, parallel quantification of multiple target molecules in a single digital PCR remains challenging. Here, we present a multiplex digital PCR method using digital melting curve analysis (digital MCA) with a SlipChip microfluidic system. The self-partitioning SlipChip (sp-SlipChip) can generate an array of nanoliter microdroplets with trackable physical positions using a simple loading-and-slipping operation. A fluorescence imaging adaptor and an *in situ* thermal cycler can be used to perform digital PCR and digital MCA on the sp-SlipChip. The unique signature melting temperature (T_m) designed for amplification products can be used as a fingerprint to further classify the positive amplification partitions into different subgroups. Amplicons with T_m differences as low as 1.5 degrees celsius were clearly separated, and multiple amplicons in the same partition could also be distinguished by digital MCA. We further demonstrated this digital MCA method with simultaneous digital quantification of five common respiratory pathogens, including *Staphylococcus aureus*, *Acinetobacter baumannii*, *Streptococcus pneumoniae*, *Hemophilus influenzae*, and *Klebsiella pneumoniae*. Since digital MCA only requires an intercalation dye instead of sequence-specific hydrolysis probes to perform multiplex digital PCR analysis, it can be less expensive and not limited to the number of fluorescence channels.

Received 21st October 2021,
Accepted 26th January 2022

DOI: 10.1039/d1an01916c

rsc.li/analyst

Introduction

This paper presents a self-partitioning SlipChip (sp-SlipChip)-based microfluidic system to perform a multiplex digital polymerase chain reaction (digital PCR) using digital melting curve analysis (digital MCA). Digital PCR can achieve absolute quantification of target nucleic acids with high sensitivity, excellent precision, and superior resolution by dividing the sample into a large number of partitions, specifically amplifying the target nucleic acid sequence, and measuring the fluorescence signal at the end-point.[1–3] A variety of microfluidic methods with different physical designs and working principles have been developed to carry out digital PCR, including pneumatic pumping,[4,5] flow partitioning,[6–9] centrifugation,[10] self-digitization,[11,12] droplet printing,[13–15] microwell compartmentalization,[16] mechanical vibration[17] and the SlipChip.[18–20] Digital PCR is becoming an essential tool for quantitative nucleic acid analysis in both life science research and clinical molecular diagnostic fields.

Although digital PCR has many advantages in quantitative nucleic acid analysis, performing multiplex digital quantification of a panel of target nucleic acid sequences in a single reaction remains challenging. Hydrolysis probes of specific nucleic acid sequences attached to different fluorophores can be applied to distinguish different amplification products to perform multiplex digital PCR.[21,22] Multiplex digital PCR can also be achieved by manipulating the concentration of fluorogenic probes of the same color.[23,24] In addition, digital PCR was demonstrated to perform multiplexed target quantification by detecting amplicons of different lengths using EvaGreen-based intercalation dye.[23] Moreover, multiplex digital PCR can also be achieved by physically dividing the microfluidic device into different sections with one section per target.[19] However, these methods can be potentially limited by the available fluorescence channels, sensitivity of the imaging sensors, and physical spaces.

MCA can also be integrated with digital PCR to perform multiplex quantification. MCA can be used to investigate nucleic acid amplification specificity and distinguish different

[a]*School of Biomedical Engineering, Shanghai Jiao Tong University, 1954 Hua Shan Road, Shanghai, China. E-mail: feng.shen@sjtu.edu.cn*
[b]*Department of Thoracic Surgery, Shanghai Chest Hospital, Shanghai Jiao Tong University, Shanghai, China*

†Electronic supplementary information (ESI) available. See DOI: 10.1039/d1an01916c

amplification products, which have unique sequences with different amplicon lengths and CG ratios. MCA utilizes general intercalation dyes, such as SYBR Green, EvaGreen and PicoGreen, as fluorescent reporters, and it can be seamlessly integrated with PCR amplification. Achieving digital MCA requires simultaneous temperature control and fluorescence analysis of a large number of reaction partitions with trackable physical locations. Digital MCA has been demonstrated to be promising for distinguishing different amplification products,[25–27] and digital MCA can also be applied to analyze the methylation level and methylation density of target nucleic acids.[28–30] However, most of these microfluidic methods still require complex instruments for the generation and manipulation of aqueous partitions, which limits the wide application of multiplex digital PCR by digital MCA.

The SlipChip is a microfluidic platform that can compartmentalize solution into a large number of reaction partitions with a simple physical slipping operation of two microfluidic plates that are in close contact, and it has been demonstrated to work for both digital PCR and digital isothermal amplification.[18,19,31,32] We previously demonstrated an sp-SlipChip that utilizes "chain-of-pearl" fluidic channels and can generate microdroplets by a surface tension-driven self-partitioning process.[33] Compared to the traditional SlipChip design, which requires precise alignment of microfeatures on different plates to establish the continuous fluidic path, sp-SlipChip has a less stringent requirement for initial assembly and loading operation.

Here, we present an sp-SlipChip to perform multiplex digital PCR quantification with EvaGreen intercalation dye by using digital MCA. The sp-SlipChip can generate 2240 of 4.5 nL droplets with trackable physical positions using a simple "loading and slipping" operation. An *in situ* thermal cycler was used to provide accurate temperature control of the sp-SlipChip. A fluorescence imaging module was developed to track the fluorescence intensity of all droplets at different temperatures in parallel. Imaging analysis software was developed to transform the fluorescence intensity measurement to a melting curve and distinguish different amplicons for multiplex digital PCR. To perform multiplex digital PCR with digital MCA on the sp-SlipChip microfluidic system, for each target nucleic acid, an amplification product with a unique melting temperature (T_m) was designed. The T_m values of different amplification products were at least 1.5 °C apart. The system can clearly distinguish different amplification products in the reaction partitions. Therefore, multiplex digital PCR quantification of different target nucleic acids can be achieved by digital MCA on an sp-SlipChip. We present the simultaneous multiplex digital PCR quantification of *Staphylococcus aureus*, *Acinetobacter baumannii*, *Streptococcus pneumoniae*, *Hemophilus influenzae*, and *Klebsiella pneumoniae* in a single digital PCR test. This method provides a low-cost and easy-to-implement multiplex digital PCR strategy with good flexibility, and it has great potential for multiplex digital nucleic acid quantification in both life science research and clinical molecular diagnostic applications.

Experimental

Materials

Plasmids and primers were synthesized by Sangon Biotech (Shanghai, China). Premix Taq was purchased from Takara Bio Inc. (Shiga, Japan). Bovine serum albumin (BSA) was purchased from Sangon Biotech (Shanghai, China). 20× EvaGreen was obtained from Biotium, Inc. (Fremont, CA). Nitric acid, ammonium fluoride, sodium hydroxide, ammonium ceric nitrate, perchloric acid, sulfuric acid, hydrogen peroxide, chloroform, acetone and ethanol were obtained from SinoPharm Chemical Reagent Co., Ltd (Beijing, China). A soda lime glass plate coated with a chromic layer and photoresist was obtained from Telic (Venture, CA). Dichlorodimethylsilane, hydrofluoric acid, and tetradecane were purchased from Aladdin Co., Ltd (Shanghai, China). Mineral oil (25 cst, 40 °C) was ordered from Innochem Technology Co., Ltd (Beijing, China). The camera of JHSM1400S-E with 14 million pixels and 8 mm fixed focus lens were purchased from Jinghang Technology Co., Ltd (Shenzhen, China). Strip blue LED lights were purchased from Cree Inc. (Shenzhen, China). 485 nm excitation wavelength filter and 522 nm emission wavelength filters were purchased from Shanghai Mega-9 Optoelectronic Co., Ltd (Shanghai, China). A Raspberry Pi 3B+ was obtained from RS Components Ltd (Shanghai, China). Power was purchased from Mean Well Switch and Power Co., Ltd (Shenzhen, China). The *in situ* thermal cycler of ETC811-Situ was purchased from Eastwin Scientific Equipments Inc. (Suzhou, China).

Fabrication of the sp-SlipChip device

The sp-SlipChip consists of a microfluidic plate containing arrays of microwells and a microfluidic plate with a "chain-of-pearl" microfluidic design. The device was fabricated by photolithography and wet etching of soda lime glass plates following a previously described protocol.[33] Prior to use, the chips needed to be cleaned with piranha solution and treated with dichlorodimethylsilane reagent according to a previous protocol[18] to make the surface hydrophobic. The surface after silanization is relatively stable. The chips can be used within one week after silanization.

Design of the fluorescence imaging module

The fluorescence imaging module was designed to acquire a series of real-time fluorescence images of the entire functional area (4 cm × 4 cm) of the sp-SlipChip during the melting curve process. The fluorescence imaging module consists of an adapter fabricated by stereo lithography appearance using photosensitive resin, a CMOS camera with a resolution of 4384 × 3288, an adjustable lens, one pair of blue LED lights, and one set of excitation and emission filters for fluorescence imaging of FAM (Carboxyfluorescein) channel (wavelength of 485 nm/522 nm) (Fig. S2†). The LEDs combined with the excitation light filter were placed symmetrically on both sides to provide the excitation light, and the incident angle was 80°. The camera and lens were fixed on the adapter and placed

6 cm above the sp-SlipChip. The camera and LED lights were controlled by a Raspberry Pi system, and the images were transferred to a computer and subjected to further fluorescence image analysis.

Single-plex digital PCR and digital MCA protocol

For single-plex digital PCR, each PCR amplification was performed in a total volume of 25 μL with 12.5 μL of Premix Taq, 1.25 μL of 20 mg mL^{-1} BSA, 1.25 μL of 20× EvaGreen, 0.5 μL of forward primer (10 μM), 0.5 μL of reverse primer (10 μM), 5 μL of template and 4 μL of ddH_2O. The primers were previously characterized[34] and are listed in Table S1.† After reaction mixture injection and droplet formation, the chip was placed on an *in situ* thermal cycler to perform digital PCR amplification. The PCR amplification protocol consisted of an initial denaturation step at 95 °C for 240 s followed by 35 cycles at 95 °C for 50 s, 62 °C for 30 s, and 72 °C for 60 s. Afterward, an MCA procedure was performed with one cycle of 95 °C for 60 s and one cycle of 40 °C for 60 s, followed by a gradual ramp-up from 70 °C to 95 °C at 0.2 °C intervals. The camera acquired images of the entire chip at 0.2 °C intervals with an exposure time of 5 s for each image acquisition. A series of temperature-dependent fluorescence images were obtained.

5-Plex digital PCR and digital MCA protocol

For 5-plex digital PCR, each PCR amplification was performed in a total volume of 25 μL with 12.5 μL of Premix Taq, 1.25 μL of BSA, 1.25 μL of 20× EvaGreen, multiplex PCR primer mixture containing the five primer sets (0.14 μM, 0.08 μM, 0.12 μM, 0.14 μM, and 0.12 μM for *S. aureus*, *A. baumannii*, *S. pneumoniae*, *H. influenzae*, and *K. pneumoniae*, respectively), five templates mixed in different proportions and ddH_2O. The amplification protocol and MCA protocol for 5-plex were the same as those for single-plex digital PCR and digital MCA.

Fluorescence image analysis

All images were processed with the same image analysis protocol. The 24-bit fluorescence images were captured. However, only the fluorescence intensity of the green channel was extracted for analysis since the fluorescence in our experiment had a wavelength of 485 nm. The bottom plate with microwells of trackable physical locations was used as a binary mask. The wells of the mask were identified as 1 and the background was identified as 0. The mask was aligned with the picture of 70 °C manually. Because the position of the chip and the droplets in the chip were fixed, all pictures were uniformly aligned to the picture of 70 °C, and the intensity of wells in each picture (temperature) was obtained. The average fluorescence intensity of each well *versus* temperature ramping was plotted to generate the melting curve. The Savitzky–Golay filter was chosen to smooth the raw curve.[35] An interquartile range method was applied to characterize the noise and define the threshold for melting peaks. Then, the derivatives of the melting curves were calculated to obtain the melting peak values, which were denoted the T_m. A histogram based on the T_m frequency of each plasmid was created, from which the five plasmids can be clearly separated by simple thresholding.

Results

We applied an sp-SlipChip device for multiplex digital PCR quantification of different target nucleic acids by digital MCA. Amplification products with different signature T_m values can be designed to differentiate different target nucleic acid sequences in the sample (Scheme 1A). The sp-SlipChip consisted of "chain-of-pearl" channels on the top plate and arrays of circular expansion wells on the bottom plate (Fig. S3†). Both plates were silanized with dichlorodimethylsilane to induce hydrophobicity on all surfaces. A thin layer of lubricating organic chemical (mineral oil : tetradecane = 1 : 1 volumetric ratio) can be placed between the two plates during device assembly. This lubricating organic chemical can not only reduce friction during the slipping operation, but also minimize aqueous vapor loss during PCR thermal cycling and MCA since the aqueous droplet is surrounded by this lubricating organic chemical that has low solubility of water. Different from the traditional digital PCR SlipChip design,[18] which requires precise microalignment of microfeatures on different plates to establish the continuous fluidic path, this "chain-of-pearl" channel enables robust fluidic loading without precise alignment. Aqueous reagents containing target nucleic acids can be introduced into the "chain-of-pearl" device with pipette loading (Scheme 1B). Then, the top plate can be moved relative to the bottom plate to overlap the "chain-of-pearl" channel with the circular expansion wells. Since there is additional void space provided by the expansion wells, the surface tension will drive the aqueous solution to self-partition into 2240 of 4.5 nL droplets (Scheme 1C). Each droplet may contain no nucleic acid template, a single type of nucleic acid template, or multiple types of nucleic acid templates. Then, the device can be placed on an *in situ* thermal cycler for PCR amplification to obtain the total number of positive wells based on the change in fluorescence intensity. A fluorescence imaging module with a FAM channel can be placed on top of the device, and MCA can be performed with an *in situ* thermal cycler (Scheme 1D and S2†). The change in fluorescence intensity with temperature was recorded and transformed into melting curves. The positive wells can be further placed into different subgroups based on their melting curves, and multiplex digital quantification of different nucleic templates can be achieved (Scheme 1E).

The sp-SlipChip can generate an array of droplets with trackable physical positions required for dMCA by a simple "load and slip" operation. The bottom plate contains an array of expansion microwells with predetermined physical positions (Fig. 1A). After the "load and slip" operations (Fig. 1B and C), aqueous droplets were constrained between the top and bottom plates with their positions fixed by the microwells on the bottom plates. A binary mask was generated based on the position of microwells on the bottom plate and overlaid

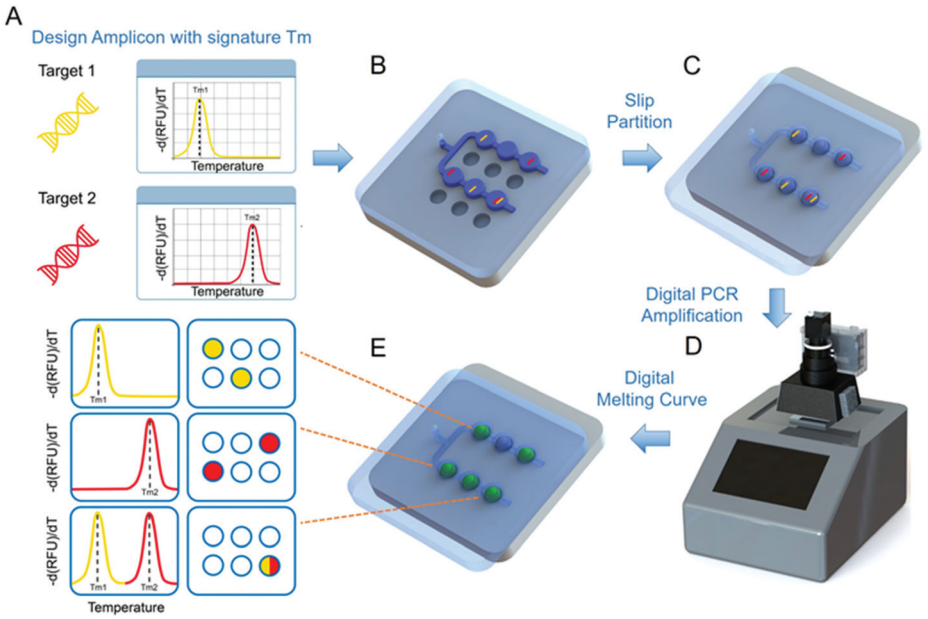

Scheme 1 Schematic drawings that demonstrate the workflow of the digital melting curve analysis (digital MCA) on the sp-SlipChip system for multiplex digital analysis. (A) Amplicons with signature T_m were designed using melting curve prediction software. (B) Top (light blue) and bottom (gray) plates of the sp-SlipChip were assembled into the loading position, and solution (dark blue) containing target molecules (red and orange) was introduced into the "chain-of-pearl" channels. (C) The top plate was slipped downward relative to the bottom plate to overlap the "chain-of-pearl" channels with an array of circular expansion wells to partition aqueous solution into an array of droplets. (D) The sp-SlipChip was placed on the *in situ* thermal cycler (dark gray) with a fluorescence imaging adaptor (black) for digital PCR and digital MCA. (E) The "positive" droplets with a significant increase in fluorescence intensity were further classified into different subgroups by digital MCA.

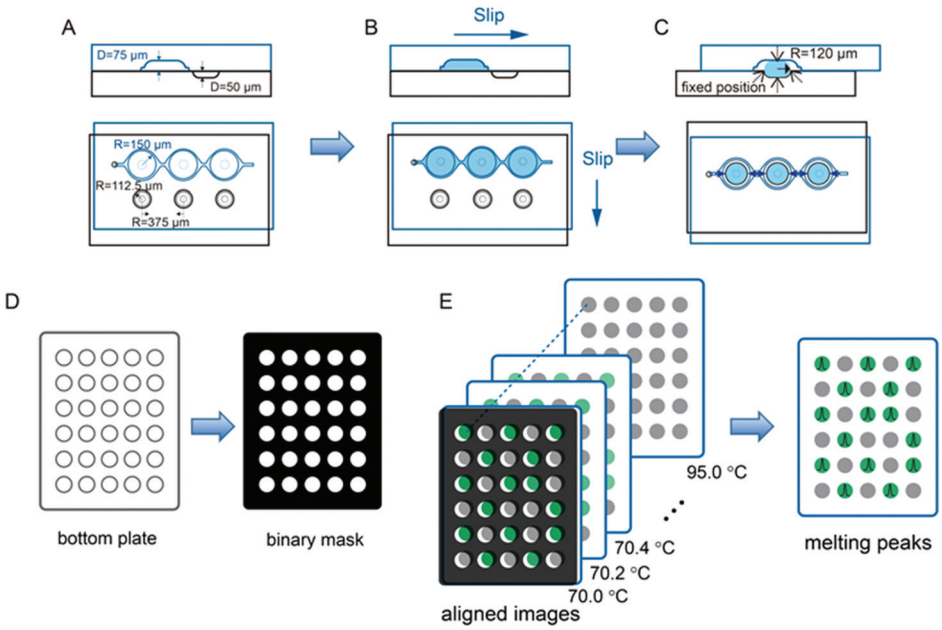

Fig. 1 Schematic drawings of droplet formation with fixed physical positions on the sp-SlipChip and the fluorescence image analysis workflow. (A) The side and top view of an assembled sp-SlipChip in the initial loading position. (B) The side and top view of the sp-SlipChip loaded with aqueous solution (light blue). (C) The side and top view of the "partitioned" position of the sp-SlipChip after the slipping process. (D) A binary mask was generated based on the position of microwells on the bottom plate. (E) All images captured during temperature rising were aligned to the binary mask and melting peaks were obtained.

with the fluorescence image of the sp-SlipChip. Since the position of the droplets is fixed, the fluorescence intensity of the droplets during the melting process (from 70.0 °C to 95.0 °C with a step of 0.2 °C) can be obtained by implementing the same binary mask, which can greatly simplify the dMCA process (Fig. 1E).

As a proof of concept, we designed the system to perform 5-plex digital PCR quantification of respiratory infectious disease-related pathogens, including *S. aureus*, *A. baumannii*, *S. pneumoniae*, *H. influenzae*, and *K. pneumoniae*. Primers were chosen to amplify target pathogens with amplification products with different signature T_m values (Table S1†). The predicted T_m values were 77.78 °C, 79.75 °C, 81.75 °C, 84.50 °C, and 90.00 °C for the amplicons of *S. aureus*, *A. baumannii*, *S. pneumoniae*, *H. influenzae*, and *K. pneumoniae*, respectively, determined by the melting curve prediction software uMELT[36] (Fig. S4†). Then, single-plex PCR amplification and MCA were performed on a Roche LC 96 real-time quantitative PCR instrument (ESI†), and the tube-based experimental melting temperatures were 78.24 ± 0.04 °C, 80.21 ± 0.02 °C, 82.23 ± 0.04 °C, 84.77 ± 0.10 °C, and 89.57 ± 0.04 °C for the *S. aureus*, *A. baumannii*, *S. pneumoniae*, *H. influenzae*, and *K. pneumoniae* amplicons, respectively (Fig. S5†). Based on the theoretical prediction and the real-time qPCR verification results, these five amplicons targeting different pathogens can be distinguished by their signature amplification product T_m values.

We first characterized the digital MCA performance with a single-plex target nucleic acid on the sp-SlipChip system.

Nucleic acids from *S. aureus*, *A. baumannii*, *S. pneumoniae*, *H. influenzae*, and *K. pneumonia* were characterized individually with the digital MCA method on the sp-SlipChip system (experimental details are in the ESI†). Briefly, the solution containing PCR master mix, one pair of primers, nucleic acid template, and EvaGreen intercalation dye was injected into the "chain-of-pearl" channel by pipetting. With one step of the slipping operation, the aqueous solution self-partitioned into an array of droplets under surface tension. The sp-SlipChip device was then placed on an *in situ* thermal cycler for PCR thermal cycling. After thirty-five cycles of PCR amplification, a melting curve analysis protocol was performed on an *in situ* thermal cycler with a fluorescence imaging adaptor. As the temperature increased from 70 °C to 95 °C, the fluorescence intensity from the positive amplification wells decreased sharply in a narrow temperature window (Fig. 2A–E). Different amplicons demonstrated a unique pattern of change in fluorescence intensity. The change in fluorescence intensity according to the change in temperature can be plotted (Fig. 2F–J), its derivative can be analyzed, and the T_m on the SlipChip can be calculated (Fig. 2K–O). For *S. aureus*, *A. baumannii*, *S. pneumoniae*, *H. influenzae*, and *K. pneumoniae*, the T_m values obtained on the SlipChip were approximately 77.77 ± 0.17 °C, 80.20 ± 0.19 °C, 81.87 ± 0.19 °C, 84.76 ± 0.19 °C, and 89.52 ± 0.21 °C, respectively (Table 1). The expected and detected concentrations of each target were listed in Table S7.† Next, we characterized this digital MCA sp-SlipChip system for analysis of the coexistence of multiple amplicons in the microwell. The solution containing PCR master mix, five pairs of primers for *S. aureus*, *A. baumannii*, *S. pneumoniae*, *H. influenzae*, and *K. pneumoniae*, EvaGreen intercalation dye, and nucleic acid templates of *S. aureus*, *A. baumannii*, *S. pneumoniae*, *H. influenzae*, and *K. pneumoniae* mixed at a 1 : 1 : 1 : 1 : 1 concentration ratio (experimental details are available in the ESI†) was injected into the "chain-of-pearl" channel by pipetting. The expected concentration of each target was approximately 36 copies per μL. Then, the solution was partitioned into droplets with a simple slipping operation. This device was placed on the digital MCA sp-SlipChip system for digital PCR amplification and digital MCA. The digital MCA sp-SlipChip system can clearly distinguish the coexistence of dual (Fig. 3A–J), triple (Fig. 3K–N), and quadruple (Fig. 3O) target amplicons by their signature melting curves. Quintuple detection of all five target amplicons was

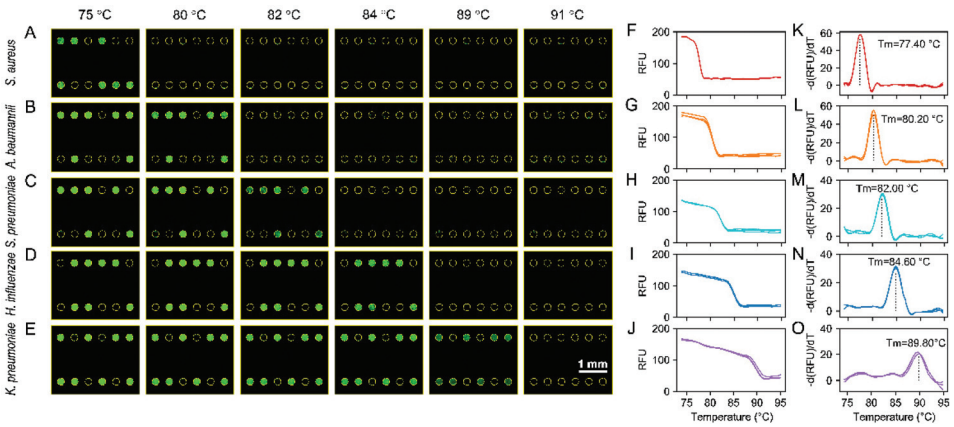

Fig. 2 Digital MCA of single-plex target nucleic acids on the sp-SlipChip system. (A–E) Magnified representative fluorescence images in FAM of digital MCA for amplicons of *S. aureus*, *A. baumannii*, *S. pneumoniae*, *H. influenzae*, and *K. pneumonia* at 75 °C, 80 °C, 82 °C, 84 °C, 89 °C, and 91 °C on different sp-SlipChip devices. (F–J) Plots represent the analyzed fluorescence intensity change respect to temperature. (K–O) The signature T_m values of amplicons by the derivative of the change in fluorescence intensity according to temperature.

Table 1 Comparison of amplicon length, amplicon GC content, calculated T_m, T_m determined by Roche, and T_m determined by the sp-SlipChip

Species	Amplicon length (bp)	Amplicon GC content (%)	T_m calc. (°C)	T_m by qPCR (°C)	Single-plex T_m by sp-SlipChip (°C)	Multiplex T_m by sp-SlipChip (°C)
S. aureus	175	34	77.75	78.24 ± 0.04	77.77 ± 0.17	78.40 ± 0.21
A. baumannii	193	38	79.75	80.21 ± 0.02	80.20 ± 0.19	80.75 ± 0.18
S. pneumoniae	110	47	81.75	82.23 ± 0.04	81.87 ± 0.19	82.23 ± 0.21
H. influenzae	168	48	84.50	84.77 ± 0.10	84.76 ± 0.19	84.78 ± 0.21
K. pneumoniae	223	60	90.00	89.57 ± 0.04	89.52 ± 0.21	89.75 ± 0.25

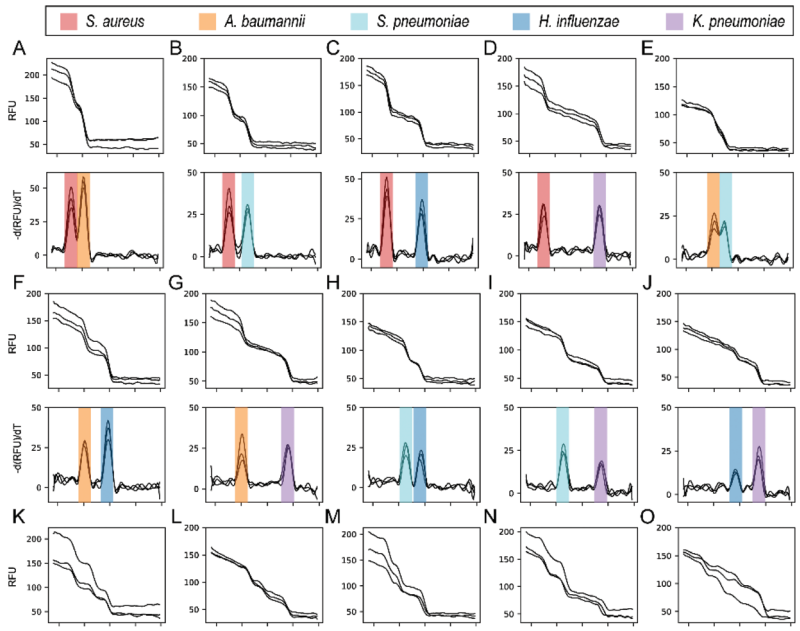

Fig. 3 Melting curve analysis for multiplex target analysis in a single amplification microwell. The different colored bars cover the melting peaks of five target nucleic acid sequences. Red, orange, cyan, blue and purple represent *S. aureus*, *A. baumannii*, *S. pneumoniae*, *H. influenzae*, and *K. pneumoniae*, respectively. (A–J) Melting curves and melting peaks for two target amplicons in a single well. (K–N) Melting curves and melting peaks for three target amplicons in a single well. (O) Melting curves and melting peaks for four target amplicons in a single well.

not observed, likely because the probability of all five templates coexisting in the same microwell was very low. No positive partition was observed in the negative control experiments. The experimental results indicate that digital MCA on the sp-SlipChip system is capable of performing multiplex nucleic acid target analysis in a single microwell.

As a proof of concept, we tested the performance of multiplex digital quantification for these five nucleic acids from *S. aureus*, *A. baumannii*, *S. pneumoniae*, *H. influenzae*, and *K. pneumoniae* by digital MCA on the sp-SlipChip. Solutions containing nucleic acids from *S. aureus*, *A. baumannii*, *S. pneumoniae*, *H. influenzae*, and *K. pneumoniae* prepared at concentration ratios of 1 : 3 : 9 : 27 : 81, 3 : 9 : 27 : 81 : 1, 9 : 27 : 81 : 1 : 3, 27 : 81 : 1 : 3 : 9, and 81 : 1 : 3 : 9 : 27 were utilized to perform multiplex digital quantification. After digital PCR and digital MCA, the amplicons of different signature melting curves could be separated into different subgroups (Fig. 4A–E), and the calculated concentrations of the five target nucleic acids agreed well with the predicted values (Fig. 4F and Tables S2–S6†). This result indicates that this digital MCA sp-SlipChip system can be used to quantify different nucleic acids in the sample through digital PCR amplification reactions with an intercalation dye.

Discussion

Digital MCA on a sp-SlipChip provides a promising method for multiplex digital PCR quantification with relatively low cost and good flexibility. This method requires universal intercalation fluorescence dyes instead of hydrolysis fluorescence probes with specific sequences; therefore, the design of multiplex amplification assays can be simplified. We have demonstrated that the system can distinguish two amplicons with a T_m difference of approximately 1.5 degrees celsius, and it can be further improved with better temperature control, advanced analysis algorithms or machine learning-based tools.[37] This method can perform a relatively large number of multiplex digital PCR quantifications, which is generally limited by the number of available fluorescence channels. This method only

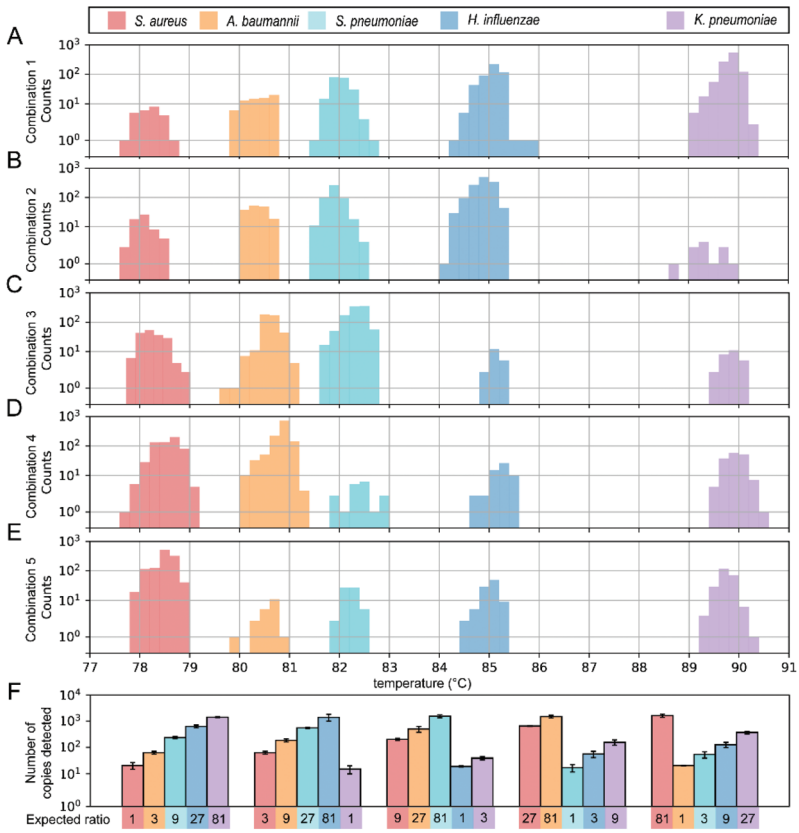

Fig. 4 Multiplex quantification of five target molecules by digital MCA on the sp-SlipChip system. (A–E) Nucleic acids from *S. aureus*, *A. baumannii*, *S. pneumoniae*, *H. influenzae*, and *K. pneumoniae* prepared at the concentration ratios of 1 : 3 : 9 : 27 : 81, 3 : 9 : 27 : 81 : 1, 9 : 27 : 81 : 1 : 3, 27 : 81 : 1 : 3 : 9, and 81 : 1 : 3 : 9 : 27. (F) Analyzed concentrations of target nucleic acids by multiplex digital PCR quantification on the sp-SlipChip system.

requires a fluorescence imaging module with an *in situ* thermal cycler, with good flexibility in the selection of thermal cycler, and it can be seamlessly integrated into laboratory practice.

The sp-SlipChip can generate an array of droplets with a simple "loading and slipping" operation, and it utilizes a surface tension-driven self-partitioning effect. No complex fluidic control instrument or cumbersome manual operation is required. This sp-SlipChip can also provide good physical separation during nucleic acid amplification and MCA. Droplet merging and cross contamination can be prevented, and the sp-SlipChip can also provide trackable physical locations for continuous monitoring of the change in fluorescence intensity during digital MCA.

To achieve clear separation of amplicons with different target T_m values, the assay may need verification and optimization on the sp-SlipChip. The concentration of primers can significantly impact the end-point signal intensity and the shape of the melting curve; therefore, in order to achieve a clear separation of different targets, it is important to verify and optimize the concentration of each primer pair (Fig. S1†). Furthermore, the melting curve may also be affected by buffer components, such as salt and detergent, and it may also be impacted by impurities introduced at the nucleic acid extraction and purification steps. Therefore, the melting curve can have small differences from the theoretical predicted value, and experimental verification of the device is necessary.

The applications of multiplex digital quantification by digital MCA can potentially be applied to a broad range of applications. This digital MCA method can be used to verify the amplification specificity of the reaction using an intercalation dye as the fluorescence indicator. This method can also be applied to analyze nucleic acid heterogeneity, such as gene mutations and methylation-related gene alterations. Additionally, the MCA method can also be potentially applied with other nucleic acid amplification methods, such as isothermal nucleic acid amplification, and can work with other unnatural nucleic acid bases, such as locked nucleic acids (LNAs).[38]

Conclusions

This paper presents a SlipChip system to perform multiplex digital PCR quantification by digital MCA with EvaGreen intercalation dye. The system utilizes an sp-SlipChip that can gene-

rate aqueous partitions for digital nucleic acid analysis with trackable physical positions. A fluorescence imaging adaptor was developed to place on top of an *in situ* thermal cycler to perform digital MCA with the sp-SlipChip. We used nucleic acids from *S. aureus*, *A. baumannii*, *S. pneumoniae*, *H. influenzae*, and *K. pneumoniae* as a representative panel. Digital MCA on the SlipChip system can identify each target individually, and multiple target amplicons in one amplification well were clearly distinguished with a melting temperature (T_m) difference as low as 1.5 °C. As a proof of concept, this sp-SlipChip system was implemented in five-plex digital PCR quantification of templates from the representative panel simultaneously. This digital MCA method on the sp-SlipChip system provides a promising strategy for multiplex digital nucleic acid quantification with a low cost, easy-to-operate workflow and good flexibility.

Author contributions

Yan Yu: methodology, investigation, writing – original draft, writing–review & editing, visualization. Ziqing Yu: methodology, investigation, writing – original draft, visualization. Xufeng Pan: methodology, writing – original draft. Lei Xu: methodology, writing – original draft. Rui Guo: investigation, writing – original draft. Xiaohua Qian: writing – original draft. Feng Shen: conceptualization, methodology, writing – original draft, writing–review & editing, visualization.

Conflicts of interest

There are no conflicts to declare.

Acknowledgements

This work is supported by the Natural Science Foundation of Shanghai (no. 19ZR1475900), the National Natural Science Foundation of China (no. 32171463, 31927803), the Innovation Research Plan supported by the Shanghai Municipal Education Commission (no. ZXWF082101), the Interdisciplinary Program of Shanghai Jiao Tong University (no. AF0820041), and the Shanghai Jiao Tong University Scientific and Technological Innovation Funds.

Notes and references

1 B. Vogelstein and K. W. Kinzler, *Proc. Natl. Acad. Sci. U. S. A.*, 1999, **96**, 9236–9241.
2 P. Liao and Y. Huang, *Micromachines*, 2017, **8**, 1–7.
3 L. Cao, X. Cui, J. Hu, Z. Li, J. R. Choi, Q. Yang, M. Lin, L. Y. Hui and F. Xu, *Biosens. Bioelectron.*, 2016, 1–15.
4 E. a. Ottesen, J. W. Hong, S. R. Quake and J. R. Leadbetter, *Science*, 2006, **314**, 1464–1467.
5 K. A. Heyries, C. Tropini, M. VanInsberghe, C. Doolin, O. I. Petriv, A. Singhal, K. Leung, C. B. Hughesman and C. L. Hansen, *Nat. Methods*, 2011, **8**, 649.
6 B. J. Hindson, K. D. Ness, D. A. Masquelier, P. Belgrader, N. J. Heredia, A. J. Makarewicz, I. J. Bright, M. Y. Lucero, A. L. Hiddessen, T. C. Legler, T. K. Kitano, M. R. Hodel, J. F. Petersen, P. W. Wyatt, E. R. Steenblock, P. H. Shah, L. J. Bousse, C. B. Troup, J. C. Mellen, D. K. Wittmann, N. G. Erndt, T. H. Cauley, R. T. Koehler, A. P. So, S. Dube, K. A. Rose, L. Montesclaros, S. Wang, D. P. Stumbo, S. P. Hodges, S. Romine, F. P. Milanovich, H. E. White, J. F. Regan, G. A. Karlin-Neumann, C. M. Hindson, S. Saxonov and B. W. Colston, *Anal. Chem.*, 2011, **83**, 8604–8610.
7 A. C. Hatch, J. S. Fisher, A. R. Tovar, A. T. Hsieh, R. Lin, S. L. Pentoney, D. L. Yang and A. P. Lee, *Lab Chip*, 2011, **11**, 3838–3845.
8 J. Park, K. G. Lee, D. H. Han, J.-S. Lee, S. J. Lee and J.-K. Park, *Biosens. Bioelectron.*, 2021, **181**, 113159.
9 M. Nie, M. Zheng, C. Li, F. Shen, M. Liu, H. Luo, X. Song, Y. Lan, J. Z. Pan and W. Du, *Anal. Chem.*, 2019, **91**, 1779–1784.
10 Z. Chen, P. Liao, F. Zhang, M. Jiang, Y. Zhu and Y. Huang, *Lab Chip*, 2017, **17**, 235–240.
11 A. M. Thompson, A. Gansen, A. L. Paguirigan, J. E. Kreutz, J. P. Radich and D. T. Chiu, *Anal. Chem.*, 2014, **86**, 12308–12314.
12 J. Yin, Z. Zou, F. Yin, H. Liang, Z. Hu, W. Fang, S. Lv, T. Zhang, B. Wang and Y. Mu, *ACS Nano*, 2020, **14**, 10385–10393.
13 W. W. Liu, Y. Zhu, Y. M. Feng, J. Fang and Q. Fang, *Anal. Chem.*, 2017, **89**, 822–829.
14 W. Zhang, N. Li, D. Koga, Y. Zhang, H. Zeng, H. Nakajima, J. M. Lin and K. Uchiyama, *Anal. Chem.*, 2018, **90**, 5329–5334.
15 Y. Pan, T. Ma, Q. Meng, Y. Mao, K. Chu, Y. Men, T. Pan, B. Li and J. Chu, *Talanta*, 2020, **211**, 120680.
16 K. Zhang, D. K. Kang, M. M. Ali, L. Liu, L. Labanieh, M. Lu, H. Riazifar, T. N. Nguyen, J. A. Zell, M. A. Digman, E. Gratton, J. Li and W. Zhao, *Lab Chip*, 2015, **15**, 4217–4226.
17 P. Xu, X. Zheng, Y. Tao and W. Du, *Anal. Chem.*, 2016, **88**, 3171–3177.
18 F. Shen, W. Du, J. E. Kreutz, A. Fok and R. F. Ismagilov, *Lab Chip*, 2010, **10**, 2666–2672.
19 F. Shen, B. Sun, J. E. Kreutz, E. K. Davydova, W. Du, P. L. Reddy, L. J. Joseph and R. F. Ismagilov, *J. Am. Chem. Soc.*, 2011, **133**, 17705–17712.
20 L. Xu, H. Qu, D. Garcia, Z. Yu, Y. Yu, Y. Shi, C. Hu, T. Zhu, N. Wu and F. Shen, *Biosens. Bioelectron.*, 2021, **175**, 112908.
21 V. Taly, D. Pekin, L. Benhaim, S. K. Kotsopoulos, D. Le Corre, X. Li, I. Atochin, D. R. Link, A. D. Griffiths, K. Pallier, B. Landi, J. B. Hutchison and P. Laurent-puig, *Clin. Chem.*, 2013, **59**, 1722–1731.
22 J. Madic, A. Zocevic, V. Senlis, E. Fradet, B. Andre, S. Muller, R. Dangla and M. E. Droniou, *Biomol. Detect. Quantif.*, 2016, **10**, 34–46.

23 Q. Zhong, S. Bhattacharya, S. Kotsopoulos, J. Olson, V. Taly, A. D. Griffiths, D. R. Link and J. W. Larson, *Lab Chip*, 2011, **11**, 2167–2174.
24 V. Taly, D. Pekin, L. Benhaim, S. K. Kotsopoulos, D. Le Corre, X. Li, I. Atochin, D. R. Link, A. D. Griffiths, K. Pallier, H. Blons, O. Bouché, B. Landi, J. B. Hutchison and P. Laurent-Puig, *Clin. Chem.*, 2013, **59**, 1722–1731.
25 P. Athamanolap, K. Hsieh, C. M. O'Keefe, Y. Zhang, S. Yang and T. H. Wang, *Anal. Chem.*, 2019, **91**, 12784–12792.
26 T. Nakagawa, J. Tanaka, K. Harada, A. Shiratori, Y. Shimazaki, T. Yokoi, C. Uematsu and Y. Kohara, *Anal. Chem.*, 2020, **92**, 11705–11713.
27 A. Moniri, L. Miglietta, K. Malpartida-Cardenas, I. Pennisi, M. Cacho-Soblechero, N. Moser, A. Holmes, P. Georgiou and J. Rodriguez-Manzano, *Anal. Chem.*, 2020, **92**, 13134–13143.
28 C. M. O'Keefe, T. R. Pisanic, H. Zec, M. J. Overman, J. G. Herman and T. H. Wang, *Sci. Adv.*, 2018, **4**, eaat6459.
29 C. M. O'Keefe, D. Giammanco, S. Li, T. R. Pisanic and T. H. J. Wang, *Lab Chip*, 2019, **19**, 444–451.
30 C. M. O'Keefe, A. M. Kaushik and T. H. Wang, *Anal. Chem.*, 2019, **91**, 11275–11282.
31 F. Shen, E. K. Davydova, W. Du, J. E. Kreutz, O. Piepenburg and R. F. Ismagilov, *Anal. Chem.*, 2011, **83**, 3533–3540.
32 M. Yu, X. Chen, H. Qu, L. Ma, L. Xu, W. Lv, H. Wang, R. F. Ismagilov, M. Li and F. Shen, *Anal. Chem.*, 2019, **91**, 8751–8755.
33 Z. Yu, W. Lyu, M. Yu, Q. Wang, H. Qu, R. F. Ismagilov, X. Han, D. Lai and F. Shen, *Biosens. Bioelectron.*, 2020, **155**, 112107.
34 L. Hu, B. Han, Q. Tong, H. Xiao and D. Cao, *Can. J. Infect. Dis. Med. Microbiol.*, 2020, **2020**, 2697230.
35 R. W. Schafer, *IEEE Signal Process. Mag.*, 2011, **28**, 111–117.
36 Z. Dwight, R. Palais and C. T. Wittwer, *Bioinformatics*, 2011, **27**, 1019–1020.
37 A. Moniri, L. Miglietta, K. Malpartida-cardenas, I. Pennisi, M. Cacho-soblechero, N. Moser, A. Holmes, P. Georgiou and J. Rodriguez-manzano, *Anal. Chem.*, 2020, **92**, 13134–13143.
38 L.-S. Chou, C. Meadows, C. T. Wittwer and E. Lyon, *BioTechniques*, 2005, **39**, 644–650.